PCCP

Accepted Manuscript

ROYAL SOCIETY OF CHEMISTRY

www.rsc.org/pccp

PCCP

RSCPublishing

ARTICLE

An improved model for predicting electrical conductance in nanochannels

Cite this: DOI: 10.1039/xoxxoooooox

M. Taghipoor,[a] A. Bertsch[a] and Ph. Renaud[a],

Received ooth January 2012,
Accepted ooth January 2012

DOI: 10.1039/xoxxoooooox

www.rsc.org/

Nanochannel conductance measurements are commonly performed to characterize nanofluidic devices Theoretical analysis and experimental investigations imply that the nanochannel conductance does not follow the macro-scale models. It is generally accepted that the conductance of nanochannels deviates from the bulk and trend to a constant value at low concentrations. In this work, we present an improved model for the nanochannel conductance that takes into account the surface chemistry of the nanochannel wall. It figured out that the nanochannel conductance is no longer constant at low concentrations. The model predictions were compared with the experimental measurements and showed a very good agreement between the model and the experiments.

Introduction

Nanofluidic transport studies in various conduits, from one and two-dimensional nanochannels to nanopore membranes and nanotubes and recently nanocapilaries, have received a growing attention for about a decade. At the nanometer scale, the fluidic transport behavior changes, mostly due to surface effects, which cannot be neglected anymore. Particularly, the electrostatic charge of the nanochannel walls has a significant impact on the molecular transport in nanometer size apertures. The charged walls attract the oppositely charged ions (counter-ions) and repel the similarly charged ones (co-ions). At low ionic concentrations, the thickness of the electrical double layer (EDL) can be of the same order as the nanochannel height or even more. As a consequence, the concentration of ions inside the nanochannel can be higher than the bulk and thus the nanochannel conductivity does not follow the expected bulk conductivity as the bulk ionic concentration decreases. Many experimental investigations have confirmed a deviation from bulk conductance for the case of nanometer size confinements[1–8].

A reliable model for nanochannel conductance is needed to predict the experimental results. It can also help to detect the probable defects in fabricated nanochannels and experimental setup. Furthermore, some of the nanofluidic devices are designed based on the nanochannel conductance variations. For example, Ion-enriched nanochannels inspired various researchers to mimic the semiconductor field-effect transistor structure in order to introduce a new tool for controlling the ionic transport in nanochannels. This led to nanofluidic field effect transistors[2] (FET) or ionic FET[8]. The development of electrical measurement of the nanochannel conductance has been widely used for the characterization of these fluidic transistors. Single molecule detection in nanoconfinement is another application that uses the nanochannel conductance measurement[8,9]. Detail knowledge of the effective ionic concentration inside nanochannels is also important if one wants to study the diffusion coefficient of charged chemical species [10].

Since the beginning of the nanofluidic studies, theoretical modeling of nanochannel conductance has been done in order to justify the results from the experiments. There have been two main approaches in nanochannel conductance calculations. The first approach uses the dependency of the electrolyte conductivity on the ionic concentration to calculate the nanochannel conductance[1,3,6,11] while the second assumes a bias electric field and calculates the ionic current due to the ionic migrations inside the nanochannel[2,5,12]. In most of the cases, the charge density inside the nanochannel was considered constant[1–3,5,7] whereas assuming a constant wall surface charge density at all ionic concentrations is a simplification that does not correspond to reality. Some studies in surface chemistry have shown that this assumption was not correct[13–16]. Also, it leads to a constant nanochannel conductance at low ionic concentrations which is not consistent with the experimental results[3,4,6].

Theoretical modeling of the surface charge density of different kinds of metal oxides has attracted some attentions for colloid chemists[17,18], geophysicist[16,19] and later in different chemical sensor studies. Yate *et al.*[17] developed a site-dissociation model

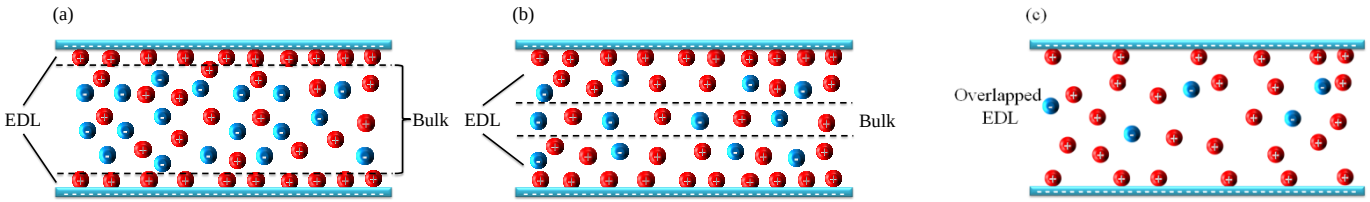

Figure 1. Schematic view of the EDL in a nanochannel. (a) At high concentration, the EDL thickness is very small and the conductance is mainly the bulk conductance. (b)When the EDL thickness gets larger, both bulk and surface-effect conductance are important. (c) At low concentrations, the EDL of walls overlap and the nanochannel conductance is only influenced by the wall surface charge.

describing the surface charge density at oxide-electrolyte interface that has been used in different fields of study. This model was utilized beside Grahame's model[20] to estimate the surface charge density and Stern layer potential in a silica porous media[15]. The surface charge density decreases while lowering the concentration[14,15] which implies that the nanochannel conductance model needs to be revised.

Similar methods was later utilized in some nanofluidic modelings[6,12,21,22]. They considered the surface chemistry of nanochannel wall and modeled the nanochannel conductance based on a non-constant wall surface charge. However, they used a variety of models for surface charge and wall electric potential. Here, we present a general model that is applicable for all kind of oxide surfaces, although we only use it for silicon dioxide.

Analytical Modeling

The conductivity of a solution containing different ions can be expressed as

$$\gamma = 10^3 N_A e \sum_i \mu_i c_i \qquad (1)$$

where μ_i ($m^2V^{-1}s^{-1}$) is the mobility of ion *i*, c_i ($mol.L^{-1}$) is the concentration of ion *i*, N_A (mol^{-1}) is the Avogadro constant, and e (C) is the electron charge. Accordingly, the conductivity of the solution inside the nanochannel depends on the concentration of ionic species, which can be different from the bulk because of the electrostatic effects of the nanochannel wall. The ratio between the thicknesses of the electric double layer (EDL) and the nanochannel height defines how the conductance of a nanochannel changes. At high concentrations where the EDL thickness is very small (Figure 1. a), the main part of the channel does not screen the surface effect. The conductivity of the solution inside the channel can be considered as the bulk's. Decreasing the ionic concentration will lead to thickening the EDL. As long as there is no EDL overlap the ions contained in the EDL screen the wall surface charge while a neutral solution is present at the center of the nanochannel (Figure 1. b). Decreasing further the ionic concentration results in an overlap of the EDL, where ions whose charge is opposite to that of the walls will fill the channel (Figure 1. c). In this condition, the nanochannel can be more conductive than the bulk, if the wall electric potential is high enough to attract more ions.

Based on equation (1), Schoch and Renaud[1] presented a model for nanochannel conductance. They assumed that the nanochannel conductance is composed of two terms. One term explained the bulk conductance and the other estimated the influence of the wall surface charge on the conductance. Their model of nanochannel conductance for a KCl solution is given as

$$G = 10^3 N_A e(\mu_{K^+} + \mu_{Cl^-})c\frac{wh}{l} + 2\mu_{K^+}\sigma_s^*\frac{w}{l} \qquad (2)$$

Where w, h, l (m) and σ_s^* $(C.m^{-2})$ are the nanochannel width, height, length and the effective wall surface charge density. The model predicts a linear bulk conductance dependence to concentration at high concentrations while the conductance reaches an offset (a plateau in log-log scale) at low concentrations. Different research groups had similar assumption in order to predict the electrical conductance of nanofluidic devices which led to a saturated conductance at low ionic concentrations[2,4,5,7,23]. Although this model has the advantage of simplicity, there is doubt as to the existence of a low concentration plateau, inspecting the experimental and numerical result reported by different research groups[1–4,6,12,24]. This encourages checking the validity of this model's assumptions and improving it.

Wall surface charge density

The assumption that has an important impact on the model is that the effective surface charge density σ_s^* is presumed to be constant for all ionic concentrations. This can be questioned since as mentioned before, the wall surface charge density changes with concentration. Some research groups has already integrated the surface chemistry models into nanofluidic governing equations in their modelings[6,12] and simulations[24]. However, a more detailed study on nanochannel surface chemistry is required.

Many publications in colloid chemistry presented methods to theoretically model the metal oxide surface charge density. The reactions at the oxide electrolyte interface that govern the surface charge density for a silicon dioxide surface are given as:

$$SiOH \overset{K_-}{\leftrightarrow} SiO^- + H_s^+ \qquad (3)$$

$$SiOH + H_s^+ \overset{K_+}{\leftrightarrow} SiH_2^+ \qquad (4)$$

Where K_- and K_+ are the equilibrium constants of the reactions. The first reaction tends to charge the oxide surface negatively, while the second reaction charges the surface positively. The concentration of the H^+ ion in the Stern layer is different from the bulk due to the electrostatic field from the wall surface charge. Assuming a Boltzmann distribution, it can be written as

$$c_{H^+}^S = c_{H^+}^B exp(\frac{-e\varphi_0}{k_B T}) \qquad (5)$$

where $c_{H^+}^B$ and $c_{H^+}^S$ are the concentration of H^+ ion in the bulk and Stern layer and k_B, T and φ_0 are the Boltzmann constant,

absolute temperature and electric potential of the Stern layer, respectively. Using the site binding model[17] and neglecting the adsorption of salt ions to the wall, the surface charge density can be expressed as

$$\sigma_s = eN_s \frac{K_+ c_{H^+}^S - \frac{K_-}{c_{H^+}^S}}{1 + K_+ c_{H^+}^S + \frac{K_-}{c_{H^+}^S}} \qquad (6)$$

where N_s $(site.m^{-2})$ is the total binding site density of the surface. Here, we neglect the adsorption of salt ions assuming the water shell around them is too large to enter the outer Helmholtz plane (OHP) and participate in a reaction. Conversely, the small H^+ ions are able to enter the OHP because of their very small ionic radius and as they are not hydrated[17].

The wall surface charge influences the ionic distribution and the electric potential in the EDL. Conversely, the wall surface charge depends on the H^+ concentration distribution, which is a function of electric potential according to equation (5). This implies that the number of equations is not enough to solve the system of equations presented above.

Grahame[20] solved the Poisson-Boltzmann equation for a symmetric electrolyte to estimate the charge density inside the diffuse layer. To this aim, he assumed a constant permittivity of the electrolyte and applied the Gauss law to the EDL. This charge density is the charge per unit area of the wall surface in $(C.m^{-2})$. For a nanochannel, it is possible to have a similar approach for both overlapping and non-overlapping EDL conditions, if the whole charged region is considered as Grahame's electric double layer. The total charge density in the charged region is then given as:

$$\sigma_t = \sqrt{8\epsilon_0 \epsilon_f k_B T n_0}\ sinh\frac{-e\varphi_0}{2k_B T} \qquad (7)$$

Where ϵ_0, ϵ_f and n_0 (m^{-3}), are the dielectric constant of vacuum, the relative dielectric constant of fluid and the number density of salt ions in the bulk, respectively.

This equation can be modified using the electroneutrality requirement of ions in the bulk for taking the pH effect into account[15]. In the modified equation the number density n_0 in equation (7) is replaced by

$$\tilde{n} = 10^3 N_A (c_0 + 10^{-pH} + 10^{pH-pKw}) \qquad (8)$$

Where c_0 is the salt concentration in the bulk, pKw is the dissociation constant of water and pH represents the bulk value. Assuming that the surface charge density of the wall should be neutralized by the oppositely charged ions, the summation of two equations (6) and (7) should be zero.

$$\sigma_t + \sigma_s = 0 \qquad (9)$$

Altogether, the Stern layer electric potential φ_0 can be calculated since both σ_t and σ_s are functions of the variable φ_0. Appling this method to a silicon dioxide nanochannel surface shows that the surface charge density increases with increasing concentrations whereas the magnitude of the electric potential of the Stern layer decreases (Figure 2). This decrease of the magnitude of Stern layer potential is related to the fact that more ions are present beside the wall. In other words, the concentration of ions close to the wall increases and according to the Gauss law, the potential decreases. This also happens in the case of a constant surface charge simulation[24]. The increase of magnitude of zeta potential at low concentrations for silica surfaces has been validated experimentally by various research teams[7,13,16]. This implies that at lower concentrations, silica surfaces better attract counter-ions due to their larger potential. However, the diffusion of counter-ions due to the concentration gradient limits the attraction toward the wall. Here, the results are obtained for a silicon dioxide surface, at room temperature, with a density of binding sites of $1.5\ sites.nm^{-2}$ and equilibrium constants $pK_+ = -0.3$ and $pK_- = -6.3$ [15]. The term ''concentration'' is used for the solvated potassium chloride concentration everywhere in the text and figures.

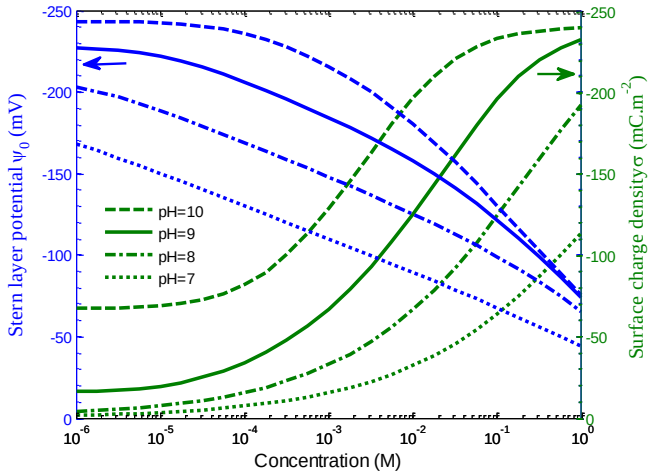

Figure 2. Surface charge density and Stern layer potential versus electrolyte concentration for different pH values for a silicon dioxide surface ($pK_- = -6.3, N_s = 1.5\ site.nm^{-2}$).The surface charge density increases with increasing salt concentrations whereas the magnitude of the electric potential of the Stern layer decreases.

Concerning the reason of the decrease in surface charge by lowering the concentration, the logarithm of the ratio between Stern layer and bulk H^+ concentration is depicted in Figure 3. At low salt concentrations, the H^+ concentration in the nanochannel is about three orders of magnitude higher than the one in the bulk for pH 7, while at high salt concentrations, this difference is even less than one order of magnitude. It means that for a negatively charged surface, the increase of H^+ concentration in the Stern layer is much higher at low ionic concentrations than at high concentrations and consequently, the wall tends to be less negatively charged according to reaction (3). The more the wall attracts H^+ ions, the more the number of negative SiO^- decreases due to surface reactions and consequently the H^+ attraction becomes weaker. Finally, there is a balance between H^+ ions attraction by the wall charge, and its surface charge density, which means that the wall surface charge is not constant for all ionic concentrations.

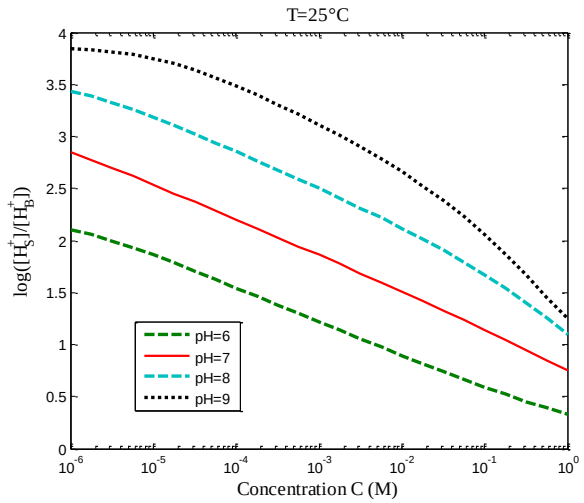

Figure 3. Evolution of the logarithm of the Stern layer to bulk H^+ concentration ratio with concentration and pH. It illustrates that for a negatively charged surface, the increase of the H^+ concentration in the Stern layer is much higher at low concentrations than at high concentrations.

Figure 4 shows the evolution of the surface charge density with the pH for different values of ionic concentration. The model predicts a maximum possible surface charge density when all the binding sites have similar charge. Higher ionic concentrations move the maximum surface charge density to lower values of the pH. The point of zero charge (PZC) is defined as the pH where the surface charge density and subsequently, the electric potential is zero. Using equations (5) and (6) the pH at the PZC is

$$pH(PZC) = -\frac{1}{2}log(K_-/K_+) \qquad (10)$$

For a silica surface, the pH of PZC corresponds to the *pH=3* which agrees with equation (10).

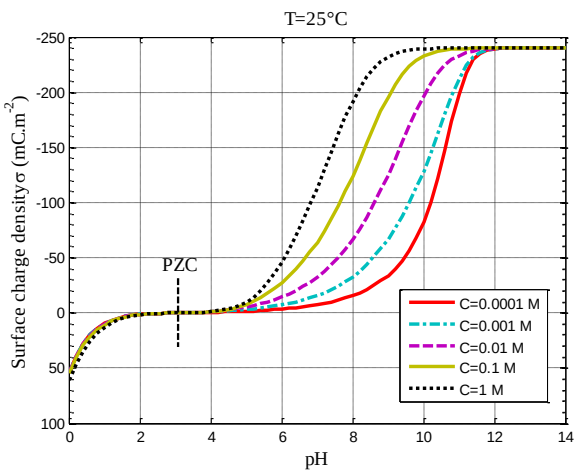

Figure 4. Evolution of the Surface charge density versus pH for different ionic concentrations for a silicon dioxide surface ($pK_- = -6.3, N_s = 1.5\ site.nm^{-2}$). The point of zero charge is at pH=3 and the maximum possible charge density is -240 mC/m^2.

Dissociated H^+ and OH^-

As it can be figured out from Figure 3, the pH of the solution in EDL is different from bulk. Considerable activity of H^+ ion inside nanochannel can affect the nanochannel conductance since its ionic mobility is higher than mobility of salt ions. Except in few works that studied the problem for acidic conditions[11,22], this effect was ignored in previous models that assumed an effect of the bulk pH only on the wall surface charge. Specially, when the salt concentration is of the same order as the ones of H^+, the effect of H^+ ion is dominant. Similarly, the role of OH^- should be considered for a positively charged wall.

For the case of a monovalent salt solution, it is possible to define an effective ionic mobility as the concentration weighted average of participating ions' mobility values. Assuming a Boltzmann distribution of all ions, the proportion of each ion concentration in the diffuse layer and in the bulk is the same. The effective ionic mobility μ_i is then defined as:

$$\mu_e = \frac{\sum \mu_i c_i^B}{\sum c_i^B} \qquad (11)$$

where μ_i and c_i^B are the ionic mobility and concentration of counter-ions in the bulk. For instance, for a negatively charged surface and a KCl solution, the effective ionic mobility is

$$\mu_e = \frac{\mu_{K^+} c_{K^+}^B + \mu_{H^+} c_{H^+}^B}{c_{K^+}^B + c_{H^+}^B} \qquad (12)$$

Where $c_{K^+}^B$ and $c_{H^+}^B$ are the bulk concentrations of K^+ and H^+ ions respectively.

The Net charge inside the nanochannel

For the nanochannel conductance to remain constant at low concentrations, the concentration of counter-ions in the nanochannel needs to remain constant. Consequently, when the bulk ionic concentration outside the nanochannel is lowered, a higher electrostatic field has to be created by the wall surface charge to attract the same amount of counter-ions in the nanochannel. This can be described using the Boltzmann distribution of ions:

$$c_i = c_i^B exp(\frac{z_i e\varphi}{k_B T}) \qquad (13)$$

where c_i, c_i^B and z_i are the concentration at specific point, bulk concentration and charge number of ion *i*. Assuming the concentration of an ion inside the nanochannel constant for different bulk concentrations, the equation (14) needs to be satisfied.

$$\frac{\widetilde{c_i^B}}{c_i^B} = exp(\frac{z_i e(\tilde{\varphi} - \varphi)}{k_B T}) \qquad (14)$$

For concentration variations of two or three orders of magnitude, the required increase of electric potential is about 4.6 and 6.9 times the ratio $k_B T/z_i e$ respectively. The ratio $k_B T/e$ is called the thermal voltage, which is about 26 mV at room temperature.

In reality, at low concentrations where the EDL overlaps, the wall surface charge density is not completely compensated inside the channel according to the results of numerical simulations[10]. In this situation, although a charged solution is present inside the nanochannel, the wall surface charge is not

neutralized inside nanochannel and a counter-ion enriched region (CER) located at the nanochannel entrance is created. In this condition, the charge density inside the nanochannel is smaller than the total wall surface charge density σ_0 and consequently, the conductance of the nanochannel is lower than when the whole surface charge densitiy of the nanochannel is neutralized. In order to model this, the Gouy-Chapmann solution for electric potential is considered to find the electric potential at the center of the nanochannel.

Assuming a Boltzmann distribution for the ions in CER provides the possibility to derive a very similar relation as equation (7) for the charge of CER. Following similar approach as for equation (7) the charge density in CER is:

$$\sigma_e = \sqrt{8\epsilon_0\epsilon_f k_B T\tilde{n}}\ sinh\frac{-e\varphi_n}{2k_B T} \quad (15)$$

where φ_n is the electric potential at the centre of the nanochannel.

Finally, the effective surface charge inside the nanochannel σ_n is given by:

$$\sigma_n = \sigma_t - \sigma_e \quad (16)$$

Figure 5 shows the evolution of the ratio of charge density inside a nanochannel to the total charge density σ_n/σ_0, with the ionic strength and pH for a silicon dioxide surface. At high concentrations, the EDL thickness is small enough to neutralize all the surface charge inside the nanochannel. At lower concentrations where the electric field cannot attract enough ions to neutralize the wall surface charge inside the channel, the ratio σ_n/σ_0 decreases. It implies that the ionic charge inside the nanochannel can differ from the wall surface charge density. The higher the pH is, the more powerful the electric field is created on the wall that can attract the counter-ions into the nanochannel.

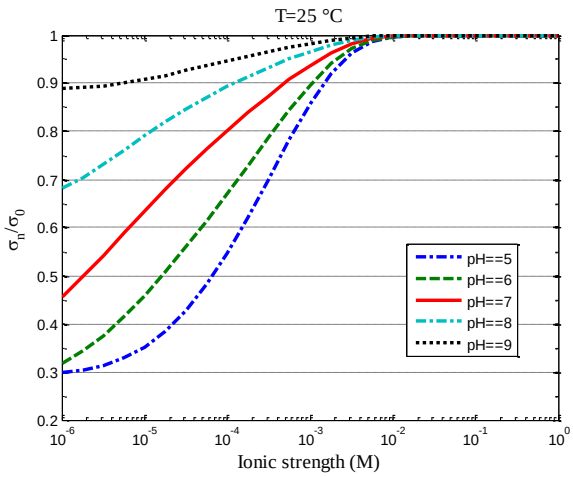

Figure 5. Evolution of the ratio of charge density inside a silica surface nanochannel to the total charge density, with the ionic strength and pH. This ratio decreases at low concentrations. It means that the surface charge density is not neutralized completely inside the nanochannel in some conditions.

The improved Model

Based on the dependency of conductivity of the solution on the ionic mobility and concentration, and applying the mentioned modifications, the improved model is developed. It is composed of two terms. The bulk term that is defined as:

$$G_B = 10^3 N_A e\frac{wh}{l}\sum_i \mu_i c_i^B \quad (17)$$

and the surface term which is defined as:

$$G_S = 2\mu_e\frac{w}{l}\sigma_n \quad (18)$$

The total conductance is the summation of both G_B and G_S.

$$G = G_S + G_B \quad (19)$$

At high ionic concentrations, the surface term has a small influence on the total conductance, the conductance is governed by channel geometry and a linear dependency of conductance to the ionic concentration is observed. At low ionic concentrations, on the other hand, the bulk term is negligible relative to the surface term and the total conductance is mainly the surface term. In fact, when decreasing the ionic concentration, the nanochannel conductance does not follow the bulk conductance nor does it reach a plateau of constant value, even if the latest case may happen in some conditions. Figure 6 shows the calculated evolution of the conductance for different values of the pH as a function of ionic concentration. When the H^+ or OH^- concentrations are higher than the electrolyte concentration, the ionic strength does not change by diluting the solution any more. In this situation, the nanochannel conductance remains constant and is not influenced by dilution. The conductance may even increase in the case of lower pH, when H^+ ions of higher ionic mobility H^+ replace the K^+ ions inside the nanochannel. Moreover, it might be possible for the case of high pH values that the electric potential rise is high enough to concentrate more salt ions since in lack of H^+ ions the surface charge does not change as much as lower pH solutions. In this case, the nanochannel conductance changes less at low concentrations.

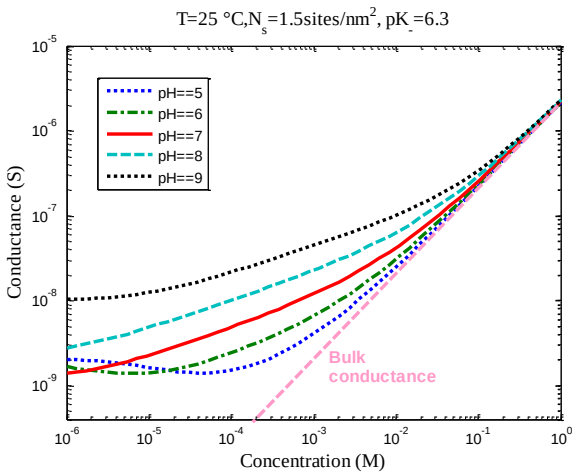

Figure 6. Conductance versus concentration for a silica surface nanochannel. The nanochannel length to width ratio is $d/w = 10$ and its height is $h = 35\ nm$. Higher surface charge density tends to a higher deviation from bulk.

In our model, the binding site density and the equilibrium constant are the parameters that define the behavior of the nanochannel walls, and its surface charge density. For the case of a silicon dioxide surface, the equilibrium constant for the creation of negatively charged sites K_- (reaction (3)) is the only equilibrium constant to take into consideration since the reported K_+ value is extremely small. In the literature, the value of pK_- is reported to be between $pK_- = 6$ and $pK_- = 7.5$ [15,24]The number of binding sites has been reported to be between $N_s = 4\ sites/nm^2$ and $N_s = 15\ sites/nm^2$ [18,19,24] for silicon dioxide. The lower limit is reported to be $N_s = 1.5\ sites/nm^2$ for a silica surface [15]. Figure 7 shows the evolution of conductance with concentration for various values of the equilibrium constant and binding site densities. A higher number of binding sites as well as higher values of equilibrium constant lead to a larger deviation from bulk line. For the range of reported values, the variation of electrical conductance is less than one order of magnitude.

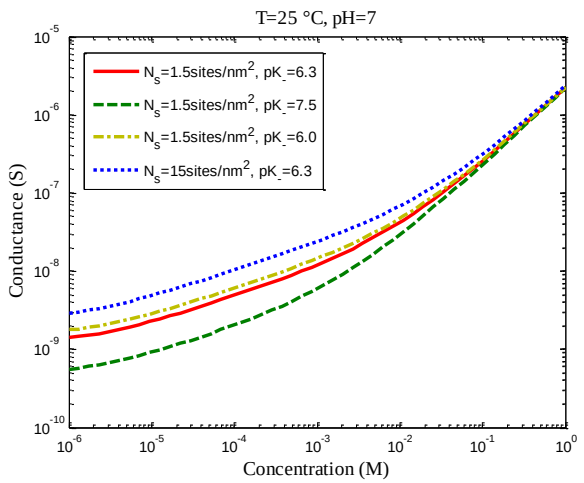

Figure 7. Conductance at *pH=7* for different surface parameters. The larger number of binding sites and larger equilibrium constant leads to higher deviation from the bulk.

Experimental validation

In Figure 8, our model is compared with the data, previously published by other research groups[1,2,6] at different pH values. Our model estimates a higher bulk conductance for the measurements at high concentration. This looks reasonable since ion-ion interactions that happen at high concentrations have been neglected. In our model, the ionic mobility reduction due to the increase of concentration[25] has not been considered, which results in an overestimation of the nanochannel conductance at high ionic concentrations. The experimental measurement of bulk conductivity (the blue circles) depicts the reduction of ionic mobility at high concentrations in Figure 8.

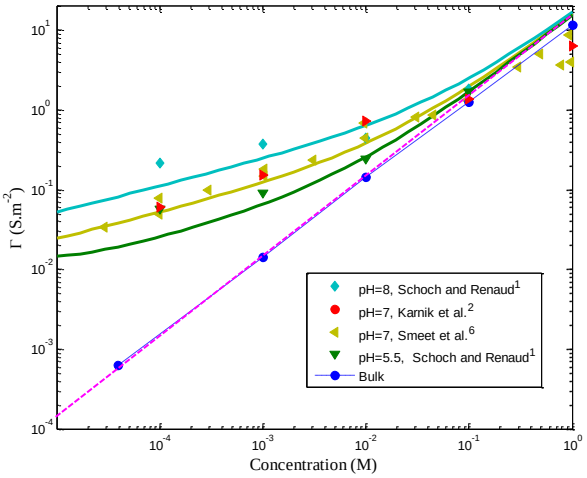

Figure 8. Comparison of our model with the data, published by other research groups[1,2,6]. Lines show the model result for corresponding pH. The modelling parameters are $N_s = 15\ sites/nm^2$ and $pK_- = 6$. The blue circles are the experimental measurements of the bulk conductivity while the pink line is a guideline for its slope regardless of the ionic mobility decrease at high concentrations.

Our model was compared with the results from controlled experiments of the electrical conductance using AC impedance measurements. The 35 *nm* nanochannels were fabricated in silicon dioxide on a fused silica substrate using a sacrificial layer approach. Figure 9.a shows a scanning electron micrograph (SEM) of a fabricated nanochannel entrance. Two platinum electrodes were embedded about 40 micrometers from the nanochannel entrances for impedance measurements (Figure 9.b). Two other platinum electrodes were placed in the microchannels for the bulk conductivity measurements. The bulk conductivity has a linear dependency on the concentration. Hence, these two electrodes can be calibrated for measuring the concentration of the solution according to a prior reference solution measurement.

(a)

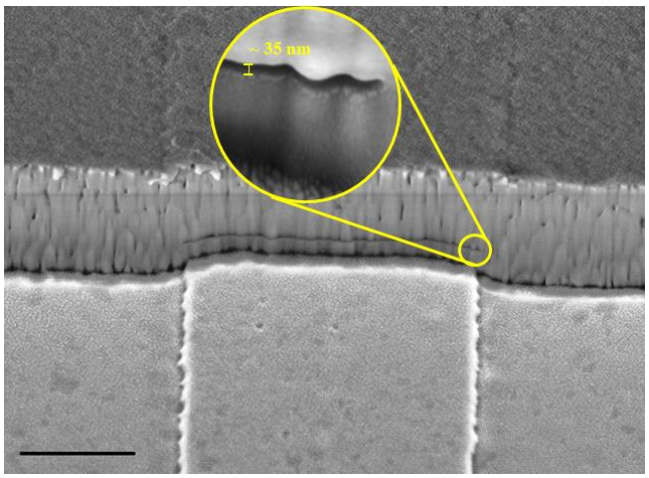

(b)

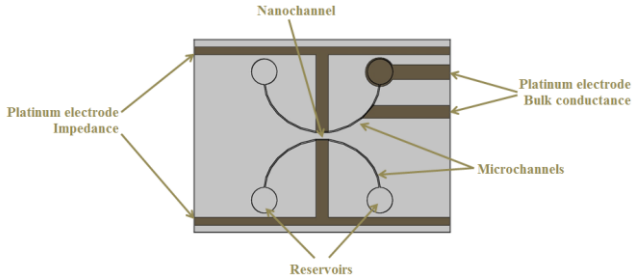

Figure 9. (a) Scanning electron micrograph (SEM) of a fabricated nanochannel entrance (view from microchannel). Scale bar 1 μm. The inset shows the nanochannel entrance with a higher magnification. The height of nanochannel is 35 nm (b) Schematic view of a device design. Platinum electrodes for impedance measurement of nanochannel are shorted in the device. Two other electrodes for measuring the bulk conductance are calibrated to assess the solution concentration.

Measurements were performed in a shielded cage and connections to the measuring instruments used coaxial cable to avoid electromagnetic noise.

Measurements were done over a large range of frequencies to find the best frequency for the nanochannel conductance measurement and discriminate it from other effects. To this aim, a computer-controlled impedance analyzer (Agilent 4294A, Agilent technologies, USA) was used in the frequency range of 40 Hz to $4MHz$.

Figure 10 shows the measurements of the electrical conductance versus the ionic concentration obtained for different designs of nanochannels (different number of nanochannels, width, length but the same height) at $pH=7$. Here, the number of binding sites is 1.5 $sites/nm^{-2}$ and $pK_{-} = 6.3$ [15]. There is a very good agreement between the model and the experiments.

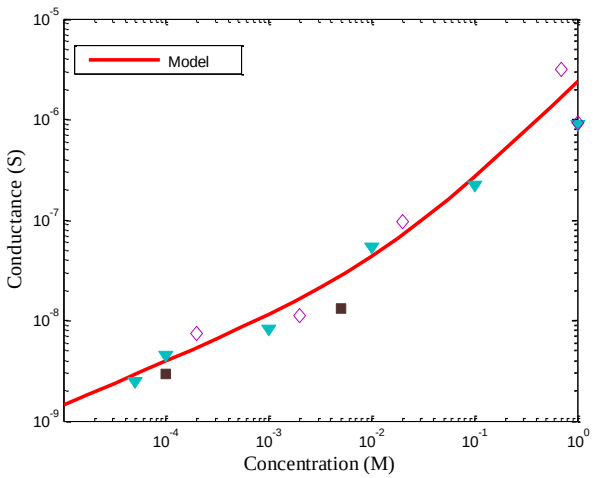

Figure 10. Nanochannel conductance versus concentration at pH = 7 for a silica surface ($pK_{-} = -6.3, N_s = 1.5$ site. nm^{-2}). The nanochannel length to width ratio is $d/w = 10$ and its height is h = 35 nm. Different symbols represent different devices.

Conclusions

We developed a new model for nanochannel conductance based on surface reactions and taking in account contribution of dissociated H+ and OH-. According to our model, the surface charge density cannot be considered constant for all concentrations. It decreases for more dilute solutions, which leads to a lower conductance of the nanochannel. Moreover, as the electric field generated by the wall surface charge fails to attract as many ions at low concentrations as for high concentrations, the nanochannel conductance is reduced even more at low concentrations. However, considering the role of H^+ ions in the nanochannel conductance results in an increase of conductance at low concentrations, due to the high ionic mobility of H^+ ions.

We compared our model with experimental measurements. There is a good agreement between experimental data and our model.

The model is capable of estimating nanochannel conductance for different physiochemical conditions of symmetric electrolytes. We plan to use the model to perform a parametric study seeking the more influential factor in nanochannel conductance.

Acknowledgements

The authors acknowledge useful discussion with Dr. S. Wu and valuable support from CMI (Center of MicroNanoTechnology) for microfabrication processes.

Notes and references

[a] Microsystems Laboratory, Ecole Polytechnique Federale de Lausanne, EPFL STI-IMT-LMIS, Station 17, 1015 Lausanne, Switzerland.
E-mail: mojtaba.taghipoor@epfl.ch

Electronic Supplementary Information (ESI) available: [details of any supplementary information available should be included here]. See DOI: 10.1039/b000000x/

References

1 R. B. Schoch and P. Renaud, *Appl. Phys. Lett.*, 2005, **86**, 253111.
2 R. Karnik, R. Fan, M. Yue, D. Y. Li, P. D. Yang and A. Majumdar, *Nano Lett.*, 2005, **5**, 943–948.
3 R. Karnik, K. Castelino, R. Fan, P. Yang and A. Majumdar, *Nano Lett.*, 2005, **5**, 1638–1642.
4 S. Wu, F. Wildhaber, O. Vazquez-Mena, A. Bertsch, J. Brugger and P. Renaud, *Nanoscale*, 2012, **4**, 5718–5723.
5 D. Stein, M. Kruithof and C. Dekker, *Phys. Rev. Lett.*, 2004, **93**, 035901.
6 R. M. M. Smeets, U. F. Keyser, D. Krapf, M.-Y. Wu, N. H. Dekker and C. Dekker, *Nano Lett.*, 2006, **6**, 89–95.
7 A. Siria, P. Poncharal, A.-L. Biance, R. Fulcrand, X. Blase, S. T. Purcell and L. Bocquet, *Nature*, 2013, **494**, 455–458.
8 S.-W. Nam, M. J. Rooks, K.-B. Kim and S. M. Rossnagel, *Nano Lett.*, 2009, **9**, 2044–2048.
9 C. Raillon, P. Cousin, F. Traversi, E. Garcia-Cordero, N. Hernandez and A. Radenovic, *Nano Lett.*, 2012, **12**, 1157–1164.

10 A. Plecis, R. B. Schoch and P. Renaud, *Nano Lett.*, 2005, **5**, 1147–1155.
11 D. C. Martins, V. Chu and J. P. Conde, *Biomicrofluidics*, 2013, **7**.
12 F. Baldessari and J. G. Santiago, *J. Colloid Interface Sci.*, 2009, **331**, 539–546.
13 D. E. Yates and T. W. Healy, *J. Colloid Interface Sci.*, 1975, **52**, 222–228.
14 J. A. Davis, R. O. James and J. O. Leckie, *J. Colloid Interface Sci.*, 1978, **63**, 480–499.
15 A. Revil and P. W. J. Glover, *Phys. Rev. B*, 1997, **55**, 1757–1773.
16 P. J. Scales, F. Grieser, T. W. Healy, L. R. White and D. Y. C. Chan, *Langmuir*, 1992, **8**, 965–974.
17 D. E. Yates, S. Levine and T. W. Healy, *J. Chem. Soc. Faraday Trans. 1 Phys. Chem. Condens. Phases*, 1974, **70**, 1807–1818.
18 R. K. Iler, *The Chemistry of Silica: Solubility, Polymerization, Colloid and Surface Properties and Biochemistry of Silica*, Wiley, 1979.
19 P. M. Reppert and F. D. Morgan, *J. Geophys. Res. Solid Earth*, 2003, **108**, 2546.
20 D. C. Grahame, *Chem. Rev.*, 1947, **41**, 441–501.
21 L.-H. Yeh, S. Xue, S. W. Joo, S. Qian and J.-P. Hsu, *J. Phys. Chem. C*, 2012, **116**, 4209–4216.
22 K. Jensen, J. Kristensen, A. Crumrine, M. B. Andersen, H. Bruus and S. Pennathur, *Phys. Rev. E*, 2011, **83**, 056307.
23 L. Bocquet and E. Charlaix, *Chem. Soc. Rev.*, 2010, **39**, 1073.
24 G. Pardon and W. van der Wijngaart, *Adv. Colloid Interface Sci.*, 2013, **199–200**, 78–94.
25 W. M. Haynes, *CRC Handbook of Chemistry and Physics, 95th Edition*, Apple Academic Press Inc., Oakville, 95, Revised., 2014.

